

Communication

Nano-Scale Rare Earth Distribution in Fly Ash Derived from the Combustion of the Fire Clay Coal, Kentucky

James C. Hower ^{1,*}, Dali Qian ^{1,2}, Nicolas J. Briot ², Eduardo Santillan-Jimenez ¹ , Madison M. Hood ^{1,3}, Ross K. Taggart ⁴ and Heileen Hsu-Kim ⁴ 

¹ Center for Applied Energy Research, University of Kentucky, 2540 Research Park Drive, Lexington, KY 40511, USA; dali.qian@uky.edu (D.Q.); esant3@uky.edu (E.S.-J.); mmho229@g.uky.edu (M.M.H.)

² Electron Microscopy Center, University of Kentucky, Lexington, KY 40506, USA; nicolas.briot@uky.edu

³ Department of Earth & Environmental Sciences, University of Kentucky, Lexington, KY 40506, USA

⁴ Department of Civil & Environmental Engineering, Duke University, Durham, NC 27708, USA; rktaggart12@gmail.com (R.K.T.); hsukim@duke.edu (H.H.-K.)

* Correspondence: james.hower@uky.edu; Tel.: +1-859-257-0261

Received: 11 March 2019; Accepted: 28 March 2019; Published: 30 March 2019



Abstract: Fly ash from the combustion of eastern Kentucky Fire Clay coal in a southeastern United States pulverized-coal power plant was studied by scanning electron microscopy (SEM), transmission electron microscopy (TEM), and selected area electron diffraction (SAED). TEM combined with elemental analysis via energy dispersive X-ray spectroscopy (EDS) showed that rare earth elements (REE; specifically, La, Ce, Nd, Pr, and Sm) were distributed within glassy particles. In certain cases, the REE were accompanied by phosphorous, suggesting a monazite or similar mineral form. However, the electron diffraction patterns of apparent phosphate minerals were not definitive, and P-lean regions of the glass consisted of amorphous phases. Therefore, the distribution of the REE in the fly ash seemed to be in the form of TEM-visible nano-scale crystalline minerals, with additional distributions corresponding to overlapping ultra-fine minerals and even true atomic dispersion within the fly ash glass.

Keywords: lanthanides; monazite; coal combustion products

1. Introduction

The enrichment and potential for extraction of the lanthanides Sc and Y, collectively rare earth elements (REE) after Connelly et al. [1], from both coal [2–7] and fly ash as well as other coal combustion products has attracted much attention in recent years [7–25]. The Pennsylvanian Fire Clay coal, primarily in its central eastern Kentucky locations, is a prime source of coal-based REE; thus, the fly ash from the combustion of the Fire Clay coal has also been of interest [9,13,17,18,26]. The Fire Clay coal owes its enrichment in REE to the emplacement of a REE-bearing-minerals volcanic ash fall parting (a tonstein) during its deposition [26].

A number of REE-bearing minerals have been found in coal; the most important REE hosts in coal include carbonate (e.g., bastnäsite [4]) and phosphate minerals (e.g., florencite, monazite, xenotime, rhabdophane, and apatite [2,10,13,27–32]). In addition to the larger, micron-scale zircon, monazite, and other REE-bearing minerals observed petrographically in coal, nano-scale REE-bearing minerals were observed in a correlative of the Fire Clay coal from Knox County, Kentucky [33]. Hower et al. [33] noted fine (10's of nm to ca. 1 μ m) monazite interspersed and interlayered with kaolinite in their transmission electron microscopy (TEM) studies of the same coal studied by Mardon and Hower [26].

The interlayered monazite–kaolinite probably originated as monazite encased in the volcanic glass, with the glass later being altered to kaolinite [30].

The modes of occurrence of REE in fly ash have been investigated by a number of authors [8,9,13,14,18,30–32]. TEM studies of central eastern Kentucky coal-sourced fly ash have shown a variety of mineral and amorphous phases to be present within the ash [18]. Indeed, in their study of a Fire Clay coal-derived fly ash, Hood et al. [18] found La and Ce in an amorphous particle. The lack of an X-ray diffraction pattern could indicate either that the region was truly a glass or that the minerals were both fine and randomly oriented within the glass, thus showing no definitive crystal structure. It has also been reported that minerals such as zircon, monazite, and xenotime in the feed coal do not melt in the boiler [34,35]; rather, minerals—such as monazite—would be shattered into much finer particles at boiler temperatures. While Hood et al. [18] also noted Y-bearing zircons in the fly ash, Hower et al. [12] found xenotime (YPO₄) in a La–Ce–Nd-monazite in a study of a ponded fly ash obtained from a blend of coals. The exact blend of coals in the latter plant is not known, but it is likely that the Fire Clay coal was included in the coals burned by the power plant in the several decades represented by the ash in the pond. In a study of the stoker ash from the Kentucky State University boiler, Hower et al. [13] noted ca. 600 × 600-nm La–Ce–Nd-bearing monazite and ca. 10-nm Ce phosphates (the orthophosphate monazite CePO₄ and the metaphosphate CeP₃O₉) attached to mullite. As with the ponded ash noted above, while the exact source of the coal was not disclosed by the stoker operator, the lanthanide + Y concentration of nearly 1200 µg/g strongly suggests that the Fire Clay coal was a major component of their burns. As with the ashes known to be sourced from the Fire Clay coal [18,26], the Kentucky State University ash has a relative enrichment in heavy REE ([13] and Figure 2 in that paper).

In this study, the fly ash from a southeastern US utility power plant burning Fire Clay coal was investigated. This sample was part of the large collection investigated for total REE contents by Taggart et al. [17] and also part of the fly ash samples analyzed for yttrium speciation by X-ray absorption spectroscopy methods [36]. While these studies provided insights on total REE contents for a wide range of fly ashes and Y-specific local coordination states, additional insights related to morphology and composition of discrete minerals would enrich our understanding of REE modes of occurrence in fly ashes of the Fire Clay coal. This contribution seeks to fill in these knowledge gaps by applying electron microscopy-based methods to study the nano-scale associations of REE with fly ash glass and mineral phases.

2. Materials and Methods

The fly ash sample KCER-93932 was obtained on 12 August 2014 from a 633-MW southeastern United States utility boiler burning eastern Kentucky Fire Clay coal. The power plant personnel assisted in the collection of the sample from the fly ash hopper (Figure 1). Moisture, ash, and carbon analyses (the latter from the ultimate analysis) were conducted at the University of Kentucky, Center for Applied Energy Research (CAER) following the appropriate ASTM international test methods, namely, D7582-15 and D3176-15 [37,38]. Major oxides and minor elements concentrations were quantified by X-ray fluorescence (XRF) at the CAER following procedures outlined by Hower and Bland [39]. The REE were extracted from the fly ash samples by an overnight 90–100 °C heated digestion with a 1:1 HF/HNO₃ acid mixture, followed by analysis via inductively coupled plasma–mass spectrometry (ICP-MS) (Agilent Technologies 7700, Agilent Technologies, Santa Clara, CA, USA) in the Department of Civil and Environmental Engineering at Duke University [17]. The accuracy of this analysis method was tested on a fly ash standard reference material (NIST SRM 1633c), which was digested and analyzed in parallel to the samples in this study. Average recoveries of individual REE elements were 89.3% to 103.4% of the Reference Concentrations (for Dy, Eu, La, Lu, Sc, and Tb) and Information Mass Concentrations (for Ce, Nd, Sm, and Yb) for SRM 1633c.

The sample for scanning electron microscopy-energy dispersive x-ray spectroscopy (SEM-EDS) was an epoxy-bound particulate pellet prepared to a 0.05 µm alumina final polish. The localization

and identification of a REE-rich particle were performed by a survey with SEM-EDS on a FEI Helios Nanolab 660 dual beam (FEI, Hillsboro, OR, USA) equipped with an Oxford Instruments X-Max^N 80 mm² EDS detector (Oxford Instruments, Abington, UK). The particle was then separated from the ash sample through focused ion beam (FIB) techniques, attached to a TEM copper grid and thinned down to electron transparency (thickness less than 100 nm). Imaging and EDS characterizations were performed on the TEM lamella using the dual beam both during and after thinning, to isolate the REE-rich region within the particle, and on a JEOL 2010F TEM at the University of Kentucky Electron Microscopy Center. Fast Fourier transform (FFT) and selected area electron diffraction (SAED) were used to determine the crystalline structure of the sub-micron grains.

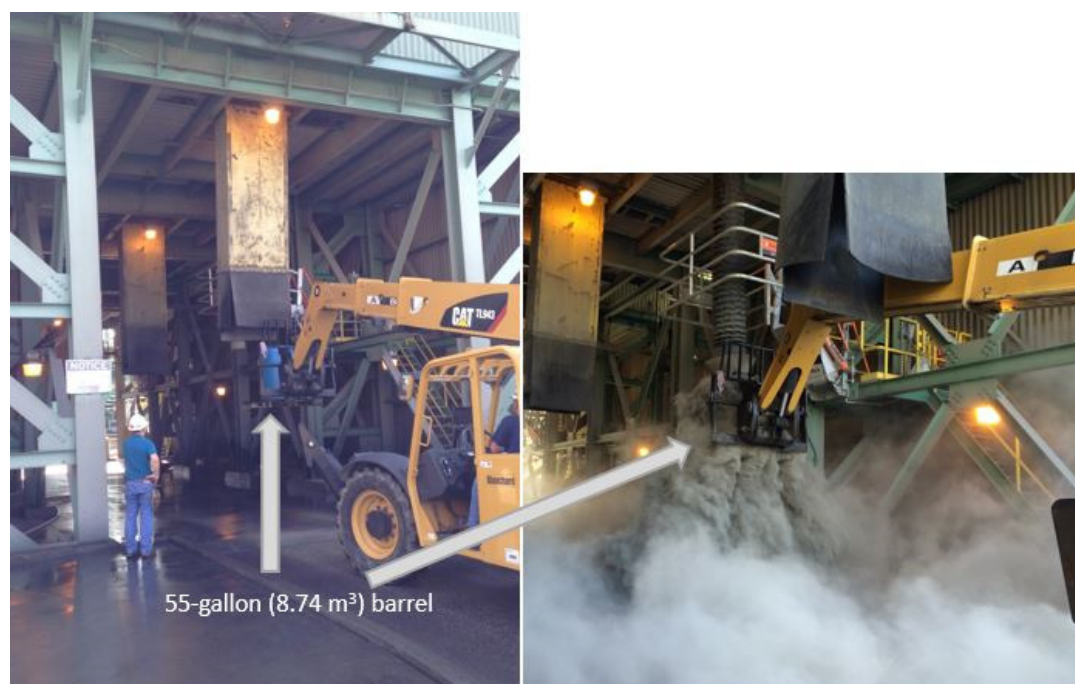


Figure 1. Filling of barrel with fly ash.

3. Results and Discussion

The whole-ash analyses of the fly ash sample KCER-93932 are reported on Table 1. The REE content of the whole ash was $669 \pm 5 \text{ mg} \cdot \text{kg}^{-1}$ (ash basis) [17]. Hower et al. [9] partially based their discussion of the partitioning of REE from the power-plant feed coal to the coal combustion fly ash on KCER-93932. Although Ba could interfere with Eu concentrations in samples with Ba/Eu >1000 [3,40], this ratio value in the sample KCER-93932 was 273, much lower than the threshold value proposed by Yan et al. [40], and, therefore, the Eu and REE concentrations could be interpreted in this work.

A spherical Al–Si-rich glass particle was identified by the preliminary SEM–EDS examination as having a relatively high rare earth content, as seen on the EDS from the region (Figure 2A). While other morphologically similar particles were observed, time and budget did not allow for the examination of REE-lean particles. An EDS scan along a beam line across the sphere demonstrated the relative abundance of Ce, Nd, Pr, and Sm in the glass (Figure 2 B–D). Adding more elements to the array showed not only the Al–Si content in the sphere, but also a P-rich grain near the lower-left edge of the sphere (Figure 2E). While the P concentration was only relatively elevated within a small portion of the scan, the REE concentration was no higher in the portion of the scan overlapping with the P-rich grain than it was elsewhere in the scan. The apparent decline in all elements towards the edge of the scan was due to the lesser analyzed volume as the edge of the spherical grain was approached.

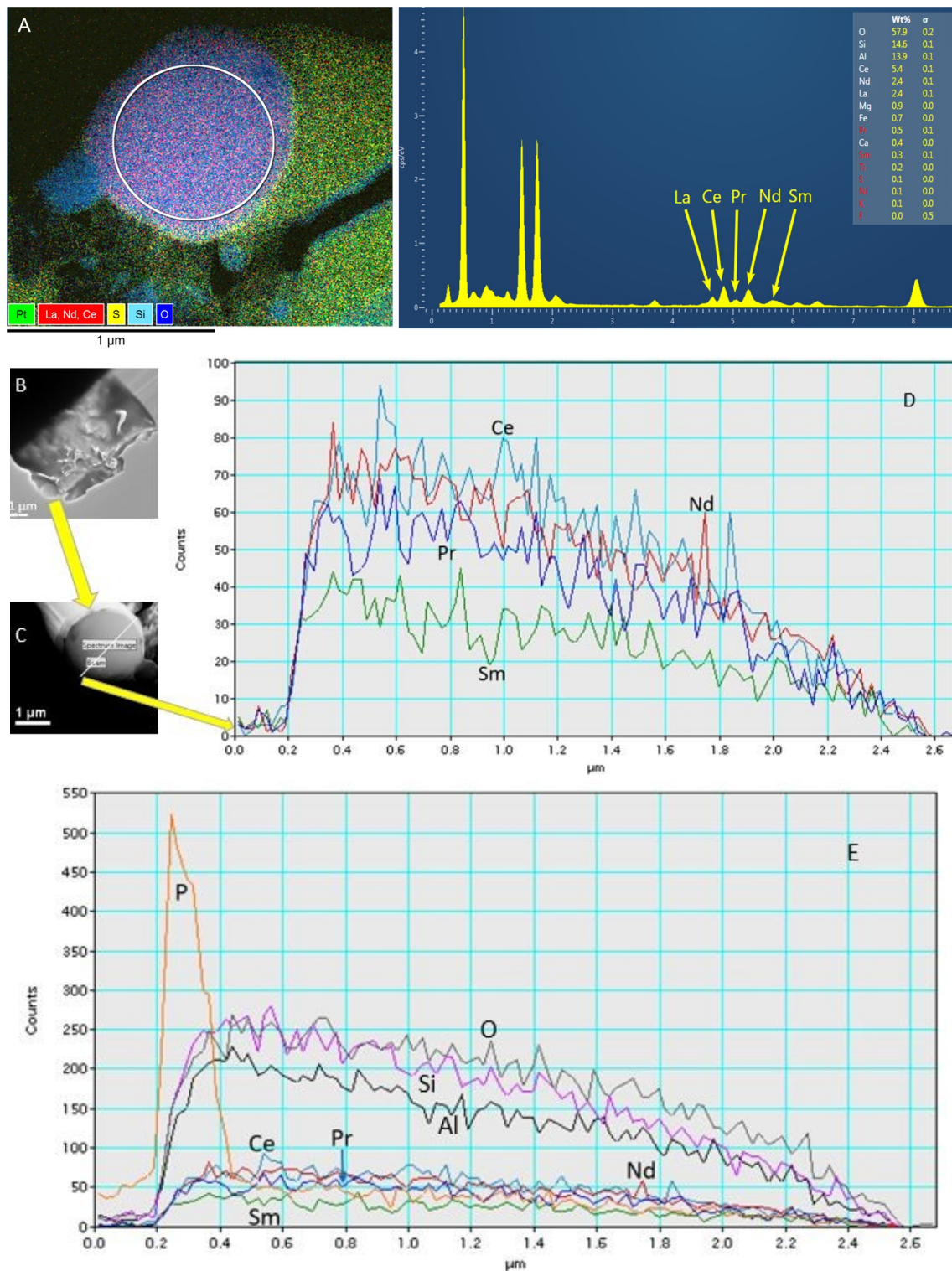


Figure 2. (A) EDS scan showing the presence of La, Ce, Pr, Nd, and Sm. (B) TEM image of the specimen from focused ion beam (FIB) liftout. (C) Expanded spectrum image of an Al-Si glass sphere with the location of beam scan indicated by the white line. (D) EDS scan across the diameter of the sphere showing relative concentrations of Ce, Nd, Pr, and Sm. (E) Enhancement of Figure 2C to show the relative concentrations of Si, Al, O, and P along with the rare earth elements shown in more detail in Figure 2D.

Table 1. Chemical analysis of fly ash sample KCER-93932. Ash and moisture (%; as received basis); carbon, hydrogen, nitrogen, sulfur, and oxygen (%; dry basis); major oxides (%; ash basis); minor elements ($\text{mg}\cdot\text{kg}^{-1}$; ash basis); Sc, Y, and rare earth elements ($\text{mg}\cdot\text{kg}^{-1}$; ash basis) (REE and minor elements, both with average and standard deviation, from Taggart et al. [17]).

	Ash	Moisture	C	H	N	S	O				
	94.25	0.17	7.76	0.42	<0.01	0.25	<0.1				
	SiO ₂	Al ₂ O ₃	Fe ₂ O ₃	CaO	MgO	Na ₂ O	K ₂ O	P ₂ O ₅	TiO ₂	SO ₃	
	54.21	28.43	7.60	4.01	1.07	0.32	2.26	0.54	1.60	0.09	
	V	Cr	Mn	Fe	Co	Ni	Cu	Zn	Ga	As	
av.	350	184	191	45,438	76	148	189	192	64	67	
std dev.	2.6	2.3	3.7	700	1.3	2.7	2.6	2.0	0.2	0.6	
	Se	Rb	Sr	Y	Mo	Ba	Pb	Th	U		
av.	7	104.31	1045	107.64	14.42	1060	87.60	34.78	16.09		
std dev.	0.6	0.77	6.1	0.29	0.20	5.79	0.10	0.36	0.07		
	Sc	La	Ce	Pr	Nd	Sm					
av.	42.39	108.25	212.20	23.66	88.13	18.68					
std dev.	0.40	1.39	2.78	0.21	0.81	0.11					
	Eu	Gd	Tb	Dy	Y	Ho	Er	Tm	Yb	Lu	
av.	3.88	18.81	2.95	17.46	107.64	3.54	9.88	1.40	8.82	1.31	
std dev.	0.03	0.17	0.02	0.12	0.29	0.01	0.06	0.01	0.02	0.02	

Note: av., average deviation; std dev., standard deviation.

Two areas were analyzed more thoroughly: Area A, near the edge of the spherical grain, and Area B, the location of the P-rich grain noted above (Figure 3). FFT imaging (Figure 4) showed a non-definitive diffraction pattern, indicating that the region was largely glassy without eliminating the possibility of small, randomly oriented minerals, as observed by Hood et al. [18] and Hower et al. [12] in their TEM studies of fly ashes. The EDS scan from area A showed the presence of Ce and Nd (Figure 5).

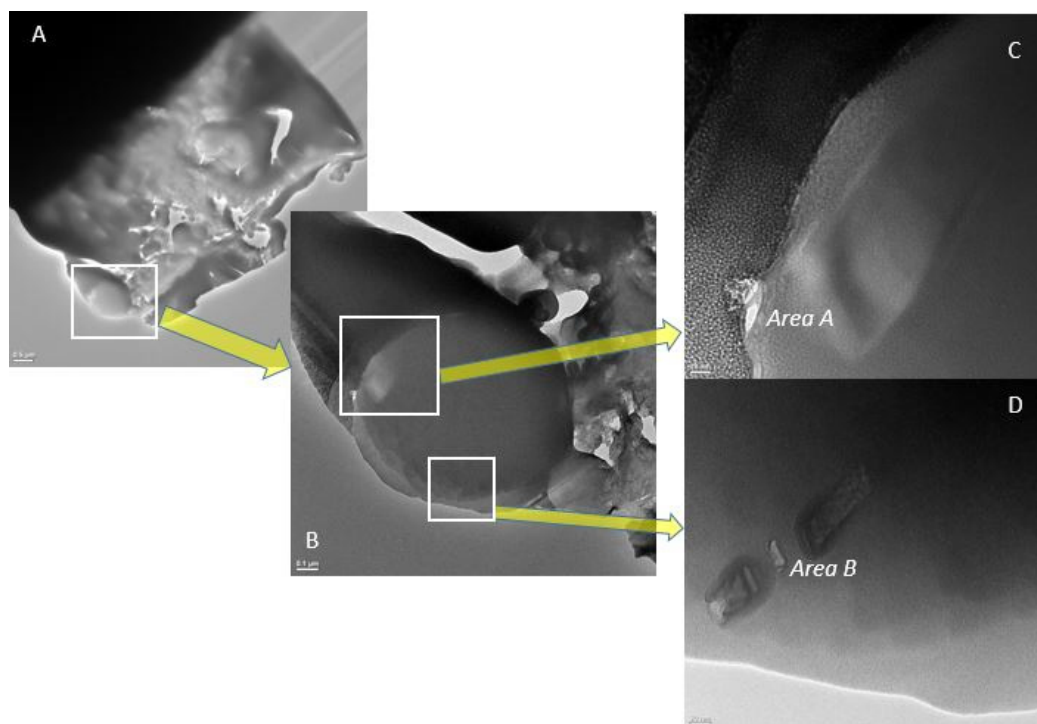


Figure 3. (A) Locations in the Al-Si glass sphere. (B) Area delimited by the white box in (A), with boxes showing the locations of area (A,B) (Figure 3C,D, respectively).

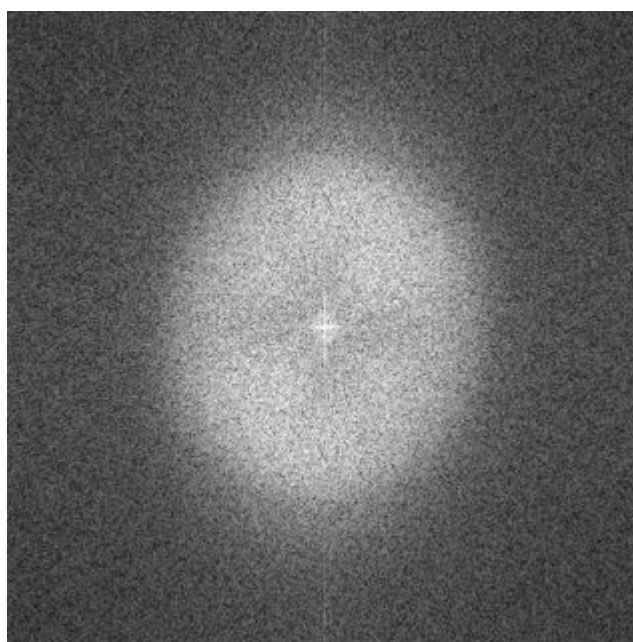


Figure 4. Fast Fourier Transform (FFT) image from area A showing non-definitive, amorphous area.

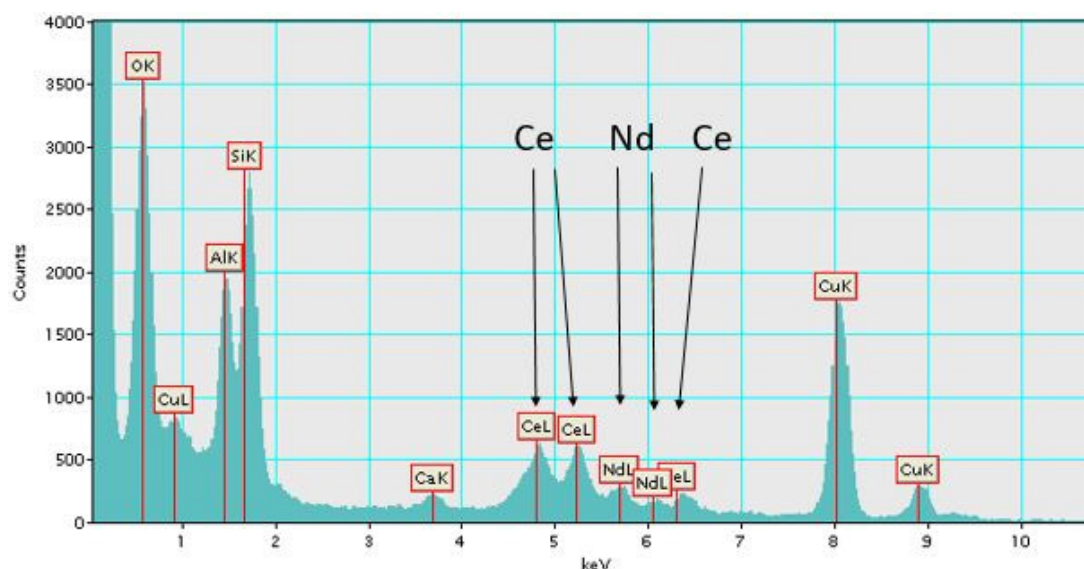


Figure 5. EDS scan of area A showing peaks corresponding to Ce and Nd.

Area B, which was associated with mineral grains, appeared more complex. Both FFT (Figure 6A) and SAED (Figure 6B) images indicated the presence of crystallinity. However, there was also an amorphous, non-crystalline surface on the mineral grain, a relic of destruction of the crystallinity by the ion beam used for FIB thinning of the specimen (right side of Figure 6C). Nevertheless, the EDS scan of the mineral showed the presence of Ce and Nd (Figure 7).

This fly ash sample was also examined by Taggart et al. [36] (denoted as “App-FA3” in that study) for Y modes of occurrence through microprobe X-ray Absorption Spectroscopy (XAS) techniques. That study also reported distinct Y species (e.g., Y distributed in glasses, YPO_4 particles), suggesting that REE occur in widely variable forms in this fly ash. We note that this previous microprobe XAS evaluated the fly ash sample at a fairly coarse spatial resolution (2 μm resolution) and was limited to a whole grain or collection of grains, rather than being performed within a grain, as shown in this study.

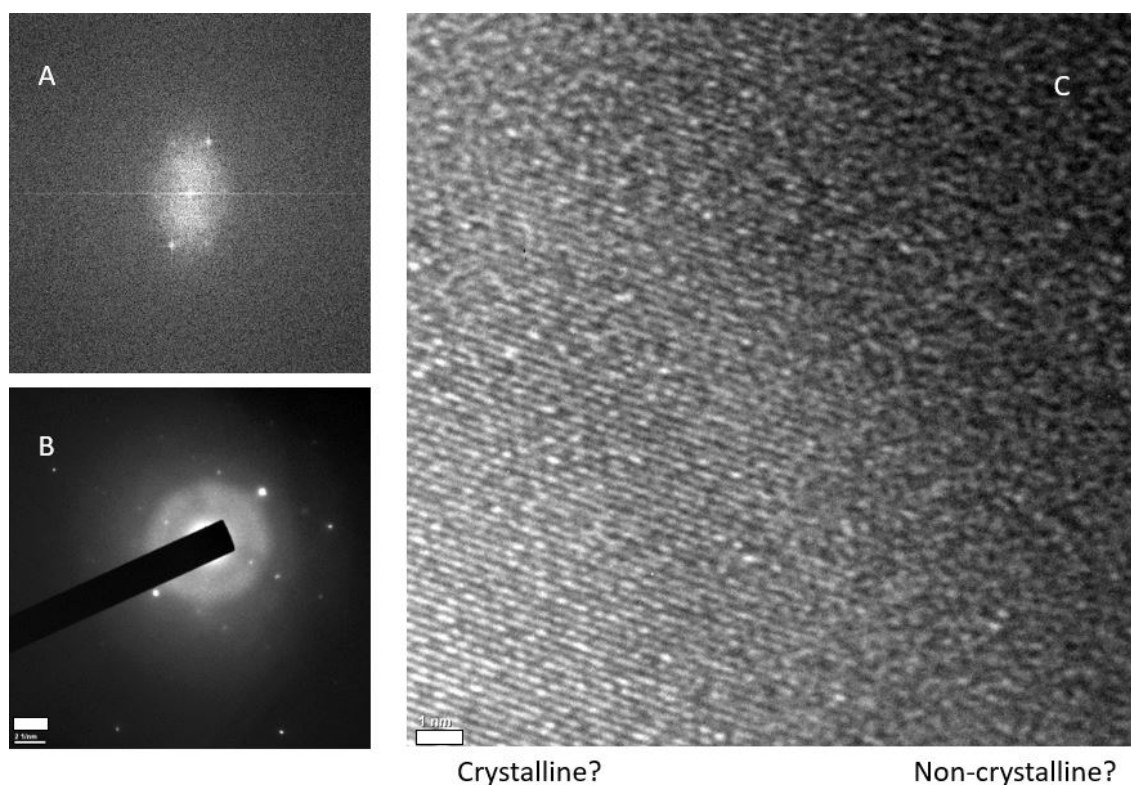


Figure 6. FFT (A) and selected area electron diffraction (SAED). (B) images of the crystalline area in the HRTEM image. The bar in the lower left corner equals 2 1/nm. (C). The scale bar in the lower-left corner of Figure 6C equals 1 nm.

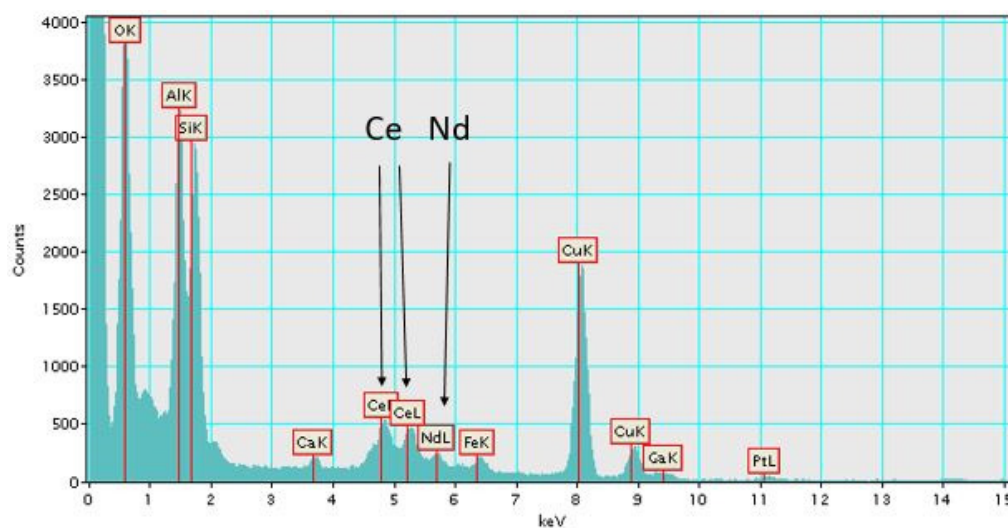


Figure 7. EDS scan of Figure 6 crystal showing the presence of Ce and Nd.

4. Conclusions

The emphasis in this study was on nano-size particles, not on a holistic view of the entire fly ash and its mix of REE-bearing and REE-lean (or absent) particles. All of the latter were scanned in the SEM–EDS examination; the sample selected for investigation was, for the sake of the study, a REE-rich area. Such a particle is not representative of the entire fly ash but, nonetheless, it is essential to understand such particles, since they are the components that collectively give this ash its reputation as a relatively REE-rich ash.

The TEM approach employed here improved the spatial resolution of other analyses, such as the bulk ICP-MS chemical analysis and the XAS approach applied by Taggart et al. [36], and subsequently revealed substantial heterogeneity of REE forms within an individual fly ash grain. Unlike the indications of minerals seen in other studies [12,13], as in the work by Hood et al. [18], the mineralogy of the particles is elusive. With the caveat that only a small, albeit REE-rich, area was investigated, this study demonstrates that REE forms in fly ash vary widely in chemical composition and size. Thus, this variability will need to be considered in the development of REE separation and extraction technologies for coal fly ash.

Author Contributions: J.C.H. was responsible for the collection of the sample; J.C.H. and M.M.H. conducted the petrographic examination of the sample; D.Q., N.J.B., and E.S.-J. were responsible for the electron beam examination; H.H.-K and R.K.T. conducted chemical and synchrotron-based studies of the fly ash; all authors participated in the writing, review, and editing of the manuscript.

Funding: This work was funded by the National Science Foundation grants CBET-1510965 and CBET-1510861 to Duke University and the University of Kentucky, respectively. Access to characterization instruments and staff assistance was provided by the Electron Microscopy Center at the University of Kentucky, supported in part by the National Science Foundation/EPSCoR Award No. 1355438 and by the Commonwealth of Kentucky.

Acknowledgments: This study was presented at the 2019 meetings of the Ohio Valley Organic Petrographers (28 March 2019; Henderson, Kentucky) and the World of Coal Ash (15 May 2019; St. Louis, Missouri). We thank editors Shifeng Dai and David French and the three reviewers for their constructive comments.

Conflicts of Interest: The authors declare no conflict of interest.

References

1. Connelly, N.G.; Hartshorn, R.M.; Damhus, T.; Hutton, A.T. (Eds.) *Nomenclature of Inorganic Chemistry: IUPAC Recommendations 2005*; Royal Society of Chemistry: Cambridge, UK, 2005; p. 366.
2. Seredin, V.V.; Dai, S. Coal deposits as a potential alternative source for lanthanides and yttrium. *Int. J. Coal Geol.* **2012**, *94*, 67–93. [[CrossRef](#)]
3. Dai, S.; Graham, I.T.; Ward, C.R. A review of anomalous rare earth elements and yttrium in coal. *Int. J. Coal Geol.* **2016**, *159*, 82–95. [[CrossRef](#)]
4. Dai, S.; Xie, P.; Jia, S.; Ward, C.R.; Hower, J.C.; Yan, X.; French, D. Enrichment of U–Re–V–Cr–Se and rare earth elements in the Late Permian coals of the Moxinpo Coalfield, Chongqing, China: Genetic implications from geochemical and mineralogical data. *Ore Geol. Rev.* **2017**, *80*, 1–17. [[CrossRef](#)]
5. Dai, S.; Xie, P.; Ward, C.R.; Yan, X.; Guo, W.; French, D.; Graham, I.T. Anomalies of rare metals in Lopingian super-high-organic-sulfur coals from the Yishan Coalfield, Guangxi, China. *Ore Geol. Rev.* **2017**, *88*, 235–250. [[CrossRef](#)]
6. Zhao, L.; Dai, S.; Graham, I.T.; Li, X.; Liu, H.; Song, X.; Hower, J.C.; Zhou, Y. Cryptic sediment-hosted critical element mineralization from eastern Yunnan Province, southwestern China: Mineralogy, geochemistry, relationship to Emeishan alkaline magmatism and possible origin. *Ore Geol. Rev.* **2017**, *80*, 116–140. [[CrossRef](#)]
7. Dai, S.; Finkelman, R.B. Coal as a promising source of critical elements: Progress and future prospects. *Int. J. Coal Geol.* **2018**, *186*, 155–164. [[CrossRef](#)]
8. Hower, J.C.; Dai, S.; Seredin, V.V.; Zhao, L.; Kostova, I.J.; Silva, L.F.O.; Mardon, S.M.; Gurdal, G. A note on the occurrence of Yttrium and Rare Earth Elements in coal combustion products. *Coal Comb. Gasific. Prod.* **2013**, *5*, 39–47.
9. Hower, J.C.; Groppo, J.G.; Henke, K.R.; Hood, M.M.; Eble, C.F.; Honaker, R.Q.; Zhang, W.; Qian, D. Notes on the potential for the concentration of rare earth elements and Yttrium in coal combustion fly ash. *Minerals* **2015**, *5*, 356–366. [[CrossRef](#)]
10. Hower, J.C.; Eble, C.F.; Dai, S.; Belkin, H.E. Distribution of rare earth elements in eastern Kentucky coals: Indicators of multiple modes of enrichment? *Int. J. Coal Geol.* **2016**, *160–161*, 73–81. [[CrossRef](#)]
11. Hower, J.C.; Granite, E.J.; Mayfield, D.; Lewis, A.; Finkelman, R.B. Notes on Contributions to the Science of Rare Earth Element Enrichment. *Minerals* **2016**, *6*, 32. [[CrossRef](#)]

12. Hower, J.C.; Groppo, J.G.; Henke, K.R.; Graham, U.M.; Hood, M.M.; Joshi, P.; Preda, D.V. Pondered and landfilled fly ash as a source of rare earth elements from a Kentucky power plant. *Coal Comb. Gasific. Prod.* **2017**, *9*, 1–21. [[CrossRef](#)]
13. Hower, J.C.; Qian, D.; Briot, N.; Henke, K.R.; Hood, M.M.; Taggart, R.K.; Hsu-Kim, H. Rare earth element associations in the Kentucky State University stoker ash. *Int. J. Coal Geol.* **2018**, *189*, 75–82. [[CrossRef](#)]
14. Blissett, R.S.; Smalley, N.; Rowson, N.A. An investigation into six coal fly ashes from the United Kingdom and Poland to evaluate rare earth element content. *Fuel* **2014**, *119*, 236–239. [[CrossRef](#)]
15. Dai, S.; Zhao, L.; Hower, J.C.; Johnston, M.N.; Song, W.; Wang, P.; Zhang, S. Petrology, mineralogy, and chemistry of size-fractionated fly ash from the Jungar power plant, Inner Mongolia, China, with emphasis on the distribution of rare earth elements. *Energy Fuels* **2014**, *28*, 1502–1514. [[CrossRef](#)]
16. Franus, W.; Wiatros-Motyka, M.M.; Wdowin, M. Coal fly ash as a resource for rare earth elements. *Environ. Sci. Pollut. Res.* **2015**, *22*, 9464–9474. [[CrossRef](#)]
17. Taggart, R.K.; Hower, J.C.; Dwyer, G.S.; Hsu-Kim, H. Trends in the rare-earth element content of U.S.-based coal combustion fly ashes. *Environ. Sci. Technol.* **2016**, *50*, 5919–5929. [[CrossRef](#)] [[PubMed](#)]
18. Hood, M.M.; Taggart, R.K.; Smith, R.C.; Hsu-Kim, H.; Henke, K.R.; Graham, U.M.; Groppo, J.G.; Unrine, J.M.; Hower, J.C. Rare earth element distribution in fly ash derived from the Fire Clay coal, Kentucky. *Coal Comb. Gasific. Prod.* **2017**, *9*, 22–33. [[CrossRef](#)]
19. Liu, J.; Dai, S.; He, X.; Hower, J.C.; Sakulpitakphon, T. Size-dependent variations in fly ash trace-element chemistry: Examples from a Kentucky power plant and with emphasis on rare earth elements. *Energy Fuels* **2017**, *31*, 438–447. [[CrossRef](#)]
20. Lin, R.; Howard, B.H.; Roth, E.A.; Bank, T.L.; Granite, E.J.; Soong, Y. Enrichment of rare earth elements from coal and coal by-products by physical separations. *Fuel* **2017**, *200*, 506–520. [[CrossRef](#)]
21. Laudal, D.A.; Benson, S.A.; Addleman, R.S.; Palo, D. Leaching behavior of rare earth elements in Fort Union lignite coals of North America. *Int. J. Coal Geol.* **2018**, *191*, 112–124. [[CrossRef](#)]
22. Zhang, W.; Honaker, R.Q. Rare earth elements recovery using staged precipitation from a leachate generated from coarse coal refuse. *Int. J. Coal Geol.* **2018**, *195*, 189–199. [[CrossRef](#)]
23. Fiket, Ž.; Medunić, G.; Furdek Turk, M.; Kniewald, G. Rare earth elements in superhigh-organic-sulfur Raša coal ash (Croatia). *Int. J. Coal Geol.* **2018**, *194*, 1–10. [[CrossRef](#)]
24. Lin, R.; Soong, Y.; Granite, E.J. Evaluation of trace elements in U.S. coals using the USGS COALQUAL database version 3.0. Part I: Rare earth elements and yttrium (REY). *Int. J. Coal Geol.* **2018**, *192*, 1–13. [[CrossRef](#)]
25. Liu, J.; Ward, C.R.; Graham, I.T.; French, D.; Dai, S.; Song, X. Modes of occurrence of non-mineral inorganic elements in lignites from the Mile Basin, Yunnan Province, China. *Fuel* **2018**, *222*, 146–155. [[CrossRef](#)]
26. Mardon, S.M.; Hower, J.C. Impact of coal properties on coal combustion by-product quality: Examples from a Kentucky power plant. *Int. J. Coal Geol.* **2004**, *59*, 153–169. [[CrossRef](#)]
27. Dai, S.; Ren, D.; Chou, C.-L.; Finkelman, R.B.; Seredin, V.V.; Zhou, Y. Geochemistry of trace elements in Chinese coals: A review of abundances, genetic types, impacts on human health, and industrial utilization. *Int. J. Coal Geol.* **2012**, *94*, 3–21. [[CrossRef](#)]
28. Dai, S.; Jiang, Y.; Ward, C.R.; Gu, L.; Seredin, V.V.; Liu, H.; Zhou, D.; Wang, X.; Sun, Y.; Zou, J.; Ren, D. Mineralogical and geochemical compositions of the coal in the Guanbanwusu Mine, Inner Mongolia, China: Further evidence for the existence of an Al (Ga and REE) ore deposit in the Jungar Coalfield. *Int. J. Coal Geol.* **2012**, *98*, 10–40. [[CrossRef](#)]
29. Dai, S.; Li, D.; Chou, C.-L.; Zhao, L.; Zhang, Y.; Ren, D.; Ma, Y.; Sun, Y. Mineralogy and geochemistry of boehmite-rich coals: New insights from the Haerwusu Surface Mine, Jungar Coalfield, Inner Mongolia, China. *Int. J. Coal Geol.* **2008**, *74*, 185–202. [[CrossRef](#)]
30. Wang, Z.; Dai, S.; Zou, J.; French, D.; Graham, I.T. Rare earth elements and yttrium in coal ash from the Luzhou power plant in Sichuan, Southwest China: Concentration, characterization and optimized extraction. *Int. J. Coal Geol.* **2019**, *203*, 1–14. [[CrossRef](#)]
31. Kolker, A.; Scott, C.; Hower, J.C.; Vazquez, J.A.; Lopano, C.L.; Dai, S. Distribution of rare earth elements in coal combustion fly ash, determined by SHRIMP-RG ion microprobe. *Int. J. Coal Geol.* **2017**, *184*, 1–10. [[CrossRef](#)]

32. Dai, S.; Zhao, L.; Peng, S.; Chou, C.-L.; Wang, X.; Zhang, Y.; Li, D.; Sun, Y. Abundances and distribution of minerals and elements in high-alumina coal fly ash from the Jungar Power Plant, Inner Mongolia, China. *Int. J. Coal Geol.* **2010**, *81*, 320–332. [[CrossRef](#)]
33. Hower, J.C.; Berti, D.; Hochella, M.F., Jr.; Mardon, S.M. Rare Earth minerals in a “no tonstein” section of the Dean (Fire Clay) coal, Knox County, Kentucky. *Int. J. Coal Geol.* **2018**, *193*, 73–86. [[CrossRef](#)]
34. Hikichi, Y.; Nomura, T. Melting temperatures of monazite and xenotime. *J. Am. Ceram. Soc.* **1987**, *70*, C252–C253. [[CrossRef](#)]
35. Quercia, G.; Perera, Y.; Tovar, H.; Rodriguez, E. Thermal degradation of zirconium silicate (ZrSiO₄) ferrules. *Acta Microscopica* **2007**, *16*, 205–206.
36. Taggart, R.K.; Rivera, N.A.; Levard, C.; Ambrosi, J.P.; Borschneck, D.; Hower, J.C.; Hsu-Kim, H. Differences in bulk and microscale yttrium speciation in coal combustion fly ash. *Environ. Sci. Process. Impacts* **2018**, *20*, 1390–1403. [[CrossRef](#)] [[PubMed](#)]
37. ASTM International. ASTM Standard D7582–15; Standard Test Methods for Proximate Analysis of Coal and Coke by Macro Thermogravimetric Analysis. In *Annual Book of ASTM Standards: Gaseous Fuels; Coal and Coke*; ASTM International: West Conshohocken, PA, USA, 2015; Section 5; Volume 05.06.
38. ASTM International. ASTM Standard D3176–15; Standard Test Methods for Ultimate Analysis of Coal and Coke. In *Annual Book of ASTM Standards: Gaseous Fuels; Coal and Coke*; ASTM International: West Conshohocken, PA, USA, 2015; Section 5; Volume 05.06.
39. Hower, J.C.; Bland, A.E. Geochemistry of the Pond Creek Coal Bed, Eastern Kentucky Coalfield. *Int. J. Coal Geol.* **1989**, *11*, 205–226. [[CrossRef](#)]
40. Yan, X.; Dai, S.; Graham, I.T.; He, X.; Shan, K.; Liu, X. Determination of Eu concentrations in 381 coal, fly ash and sedimentary rocks using a cation exchange resin and inductively coupled 382 plasma mass spectrometry (ICP-MS). *Int. J. Coal Geol.* **2018**, *191*, 152–156. [[CrossRef](#)]



© 2019 by the authors. Licensee MDPI, Basel, Switzerland. This article is an open access article distributed under the terms and conditions of the Creative Commons Attribution (CC BY) license (<http://creativecommons.org/licenses/by/4.0/>).